© 2015. Published by The Company of Biologists Ltd | Journal of Cell Science (2015) 128, 2541-2552 doi:10.1242/jcs.171652

RESEARCH ARTICLE

The small GTPase Rab8 interacts with VAMP-3 to regulate the delivery of recycling T-cell receptors to the immune synapse

Francesca Finetti[1], Laura Patrussi[1], Donatella Galgano[1], Chiara Cassioli[1], Giuseppe Perinetti[2], Gregory J. Pazour[3] and Cosima T. Baldari[1,*]

ABSTRACT

IFT20, a component of the intraflagellar transport (IFT) system that controls ciliogenesis, regulates immune synapse assembly in the non-ciliated T-cell by promoting T-cell receptor (TCR) recycling. Here, we have addressed the role of Rab8 (for which there are two isoforms Rab8a and Rab8b), a small GTPase implicated in ciliogenesis, in TCR traffic to the immune synapse. We show that Rab8, which colocalizes with IFT20 in Rab11$^+$ endosomes, is required for TCR recycling. Interestingly, as opposed to in IFT20-deficient T-cells, TCR$^+$ endosomes polarized normally beneath the immune synapse membrane in the presence of dominant-negative Rab8, but were unable to undergo the final docking or fusion step. This could be accounted for by the inability of the vesicular (v)-SNARE VAMP-3 to cluster at the immune synapse in the absence of functional Rab8, which is responsible for its recruitment. Of note, and similar to in T-cells, VAMP-3 interacts with Rab8 at the base of the cilium in NIH-3T3 cells, where it regulates ciliary growth and targeting of the protein smoothened. The results identify Rab8 as a new player in vesicular traffic to the immune synapse and provide insight into the pathways co-opted by different cell types for immune synapse assembly and ciliogenesis.

KEY WORDS: Rab8, TCR recycling, Immune synapse

INTRODUCTION

T-cell activation is initiated by engagement of the antigen receptor (T-cell receptor, TCR) following an encounter with an antigen-presenting cell (APC) bearing cognate peptide–major-histocompatibility-complex (pMHC). This event triggers a profound redistribution of membrane-associated receptors and intracellular signaling mediators that eventually leads to the formation of a stable, highly structured interface between the T-cell and APC known as the immune synapse (Fooksman et al., 2010). Naive T-cell commitment to become activated and differentiate to an effector or memory cell is crucially dependent on sustained signaling at the immune synapse (Iezzi et al., 1998). This is achieved by the steady recruitment of new TCRs to the immune synapse as engaged receptors undergo internalization. A number of mechanisms cooperate to ensure a long-lasting supply of TCRs to the immune synapse, including the passive and actin-dependent clustering of surface TCR complexes and the polarized delivery to the immune synapse of TCR complexes from a pool associated with recycling endosomes (Das et al., 2004).

[1]Department of Life Sciences, University of Siena, Siena 53100, Italy. [2]Department of Medical, Surgical and Health Sciences, School of Dentistry, University of Trieste, Trieste 34129, Italy. [3]Program in Molecular Medicine, University of Massachusetts Medical School, Worcester, MA 01605, USA.

*Author for correspondence (cosima.baldari@unisi.it)

Received 16 March 2015; Accepted 22 May 2015

Although the TCR has long been known to recycle, the trafficking machinery that orchestrates TCR recycling has as yet not been fully elucidated. The TCR has been shown to associate with the Rab11$^+$ pericentrosomal endosome compartment, as well as with Rab4$^+$ endosomes (Kumar et al., 2011; Liu et al., 2000), indicating that it uses both the slow and the fast recycling pathways to return to the cell surface. Moreover the TCR can be found in endosomes marked by Rab35 and its GAP EPI64C (Patino-Lopez et al., 2008). We have recently demonstrated that IFT20, a component of the intraflagellar transport (IFT) system that is responsible for the assembly and maintenance of cilia and flagella (Pazour and Bloodgood, 2008; Pedersen and Rosenbaum, 2008), is a central regulator of the pathway that regulates TCR recycling (Finetti et al., 2009), interacting with Rab5 to promote TCR trafficking from early endosomes (Finetti et al., 2014).

In ciliated cells the directional transport of specific receptors to the ciliary membrane is promoted by Rab8 (which has two isoforms, Rab8a and Rab8b), a ubiquitous GTPase that has been mainly studied in polarized cells where it has been shown to associate with macropinosomes, vesicles and tubules to promote receptor recycling to membrane ruffles at the leading edge, in concert with Rab11 and Arf6 (Hattula et al., 2006). Moreover, Rab8 participates in recycling of the α-amino-3-hydroxy-5-methyl-4-isoxazolepropionic acid (AMPA) receptors to the dendritic spine surface as well as in the intracellular transport of the metabotropic glutamate receptor type 1 in neuronal cells (Esseltine et al., 2012; Gerges et al., 2004). Rab8 is activated at the base of the cilium by its guanine nucleotide exchanger Rabin8 (also known as RAB3IP), where it is recruited by the BBSome, a multimolecular complex that cooperates with the IFT system in the ciliary trafficking of membrane proteins (Liew et al., 2014; Nachury et al., 2007; Wei et al., 2012). A functional link between Rab8 and the recycling compartment in ciliated cells has been established with the finding that Rabin8 interacts with GTP-bound Rab11 and is carried to pericentrosomal Rab8 by Rab11$^+$ vesicles, in association with the TRAPPII complex (Westlake et al., 2011). Hence, in ciliated cells Rab8 appears to couple endosome recycling to ciliary trafficking.

Based on the similarities between the immune synapse and the primary cilium, as well as on a recent report showing that Rab8 colocalizes with TCR$^+$ endosomes in T-cells (Soares et al., 2013), here we have addressed the potential implication of Rab8 in TCR recycling and its interplay with IFT20 in this process. The results provide evidence that Rab8 acts as a new regulator of TCR recycling downstream of IFT20 by recruiting the vesicular (v)-SNARE VAMP-3, a function that is co-opted by ciliated cells to promote ciliary growth and ciliary targeting of the protein smoothened (Smo). We also provide evidence that the transferrin receptor (TfR) and the chemokine receptor CXCR4, both of which undergo polarized recycling to the immune synapse, are regulated by

Journal of Cell Science (2015) 128, 2541-2552 doi:10.1242/jcs.171652

pathways that differ in their respective requirement for Rab8 and IFT20, highlighting the combinatorial usage of specific regulators of membrane trafficking in the orchestration of receptor recycling in T-cells.

RESULTS

Rab8 colocalizes with Rab11 and IFT20 at a pericentrosomal compartment in T-cells

The localization of Rab8 was analyzed by confocal microscopy of Jurkat T-cells as well as primary human peripheral blood T-cells. Rab8 was found to be mostly associated with a pericentrosomal compartment, similar to in ciliated cells (Fig. 1A,B). Colocalization analyses revealed a significant overlap of the Rab8 staining with Rab11 (Fig. 1A,B), suggesting its association with recycling endosomes. In support of this notion, fractionation of cell membranes by iodixanol gradient centrifugation showed that Rab8 was present together with Rab11 in the low-density fractions, which are enriched in recycling endosomes, but not in the high-density fractions enriched in late endosomes or lysosomes, as shown by immunoblotting with anti-Rab7 antibodies (Fig. 1C).

We have recently shown that IFT20 colocalizes in part with Rab11 in T-cells (Finetti et al., 2014), raising the possibility that IFT20 and Rab8 might associate at Rab11^{+} endosomes. Immunofluorescence analysis showed indeed a significant colocalization of IFT20 with Rab8 (Fig. 1A,B), supporting the hypothesis that Rab8 might interface with IFT20 to control TCR recycling.

Rab8 participates in the IFT20-dependent pathway of TCR recycling

The involvement of Rab8 in TCR recycling was addressed on Jurkat T-cells as well as primary T-cells transiently transfected with either wild-type Rab8 or its dominant-negative (DN-Rab8) T22N mutant. To measure recycling, we used an antibody-based assay to selectively track the receptors that had been engaged at the plasma membrane. T-cells were incubated with anti-CD3 monoclonal antibody (mAb) to induce TCR internalization. Internalized receptors were then allowed to recycle to the cell surface, where they were identified by flow cytometry using fluorochrome-labeled secondary antibodies. Alternatively, cells were fixed and permeabilized and the internalized receptors were visualized by confocal microscopy after labeling with secondary antibodies.

Expression of DN-Rab8 resulted in a profound impairment in TCR recycling, as assessed by flow cytometry (Fig. 2A; Fig. 3A). Consistent with this defect, imaging of the internalized receptors showed a significant accumulation of endosomes containing internalized TCRs in cells expressing DN-Rab8 compared to cells transfected with empty vector or a construct encoding wild-type Rab8 (Fig. 2B). In support of Rab8 being involved in TCR recycling, recycling was enhanced when cells were transfected with a constitutively active (CA-Rab8) mutant, as shown both by flow cytometric analysis and by imaging the endosomes containing internalized TCRs (Fig. 2A,B).

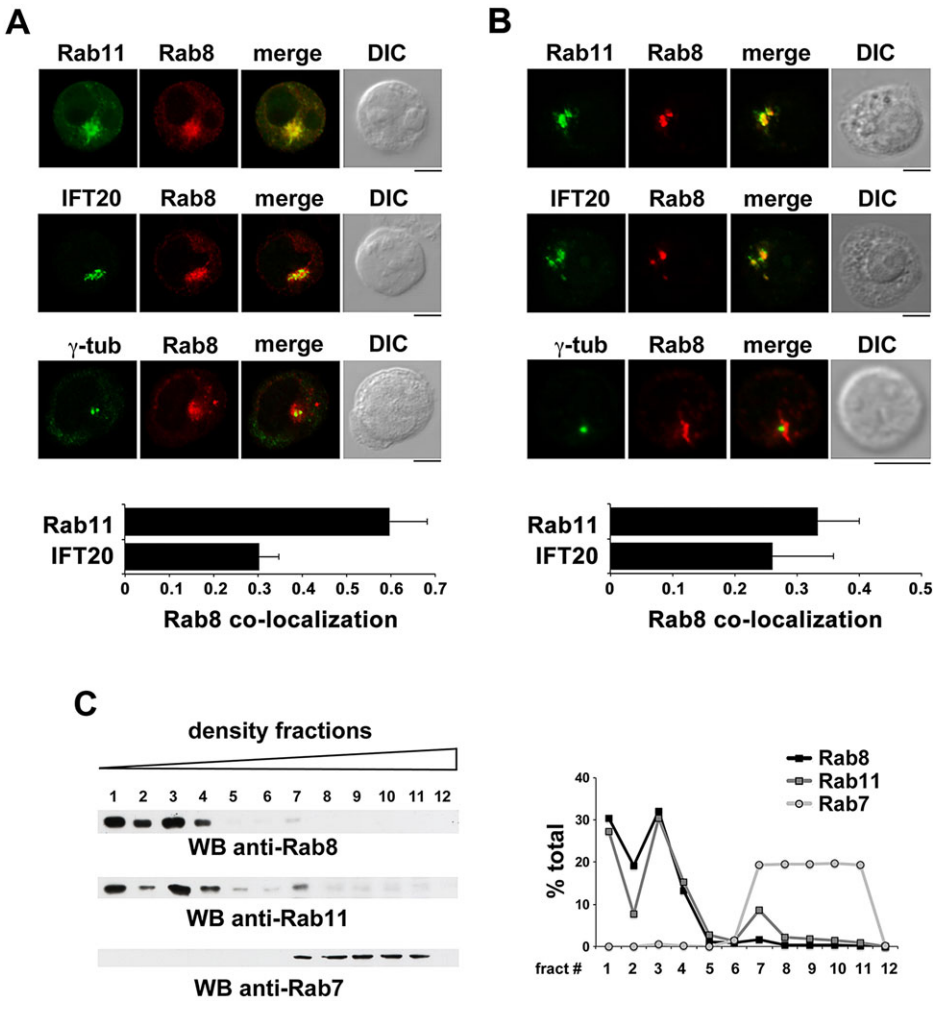

Fig. 1. Rab8 colocalizes with Rab11 and IFT20 in T-cells. (A,B) Quantification (mean±s.d.) of the weighted colocalization of Rab8 with Rab11 or IFT20 in Jurkat cells (A) or primary T-cells (B). At least 20 Jurkat cells and 20 T-cells were analyzed for each marker ($n \geq 3$). Representative images (medial optical sections) are shown. Scale bars: 5 µm. (C) Representative immunoblot analysis of Jurkat cell membranes fractionated on 10–30% iodixanol gradients. Immunoreactive bands were quantified using ImageJ and plotted as specific protein in each fraction versus total specific protein ($n \geq 3$).

Journal of Cell Science

Journal of Cell Science (2015) 128, 2541-2552 doi:10.1242/jcs.171652

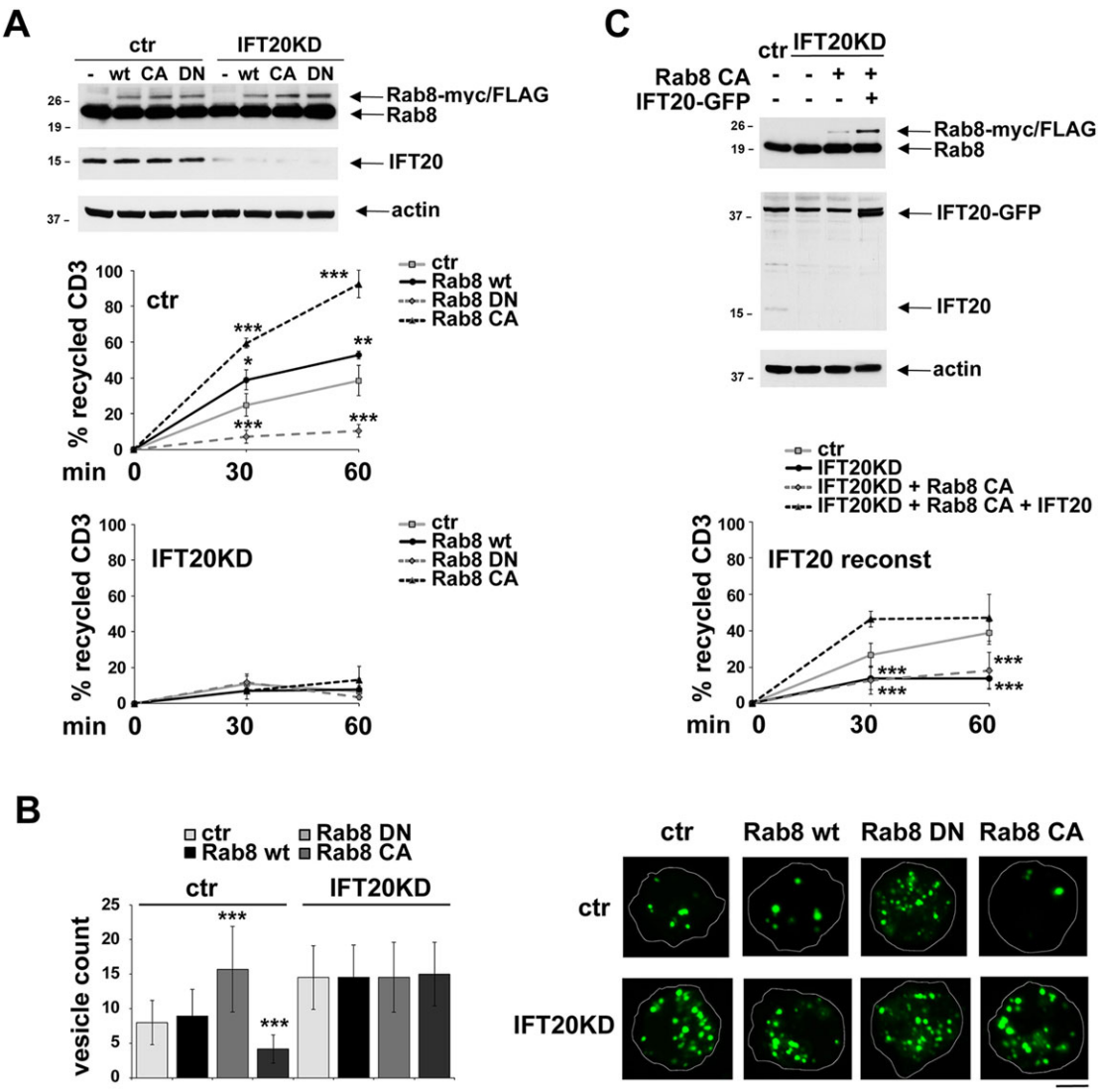

Fig. 2. Rab8 is required for TCR recycling downstream of IFT20. (A) Flow cytometric analysis of TCR recycling in control and IFT20KD Jurkat cells, transiently transfected with either empty vector (ctr), or wild-type Rab8 (wt), dominant-negative Rab8 (DN) or constitutively active Rab8 (CA), all tagged with Myc and FLAG. A construct encoding GFP under the control of a constitutive promoter was included in each transfection as a control. Analyses were carried out at 24 h post-transfection, gating on GFP^+ live cells. The data, which for each time point refer to triplicate samples from three independent experiments, are presented as the percentage of internalized receptors that have recycled to the cell surface (mean±s.d.). A representative immunoblot showing endogenous and recombinant Rab8 expression and documenting IFT20 depletion in the IFT20KD samples is included. (B) Counts of vesicles containing internalized CD3 in control and IFT20KD Jurkat cells transiently transfected with vector control (ctr), wild-type Rab8 or the respective Rab8 mutants. At least 60 cells were analyzed for each marker ($n \geq 3$). The data are presented as number of labeled vesicles in individual medial confocal sections (mean±s.d.). Objects smaller than 0.005 μm^2, as well as the compact pericentrosomal aggregate, were excluded from the analysis. At least 20 cells were analyzed for each receptor ($n \geq 3$). Representative images are shown on the right. Scale bar: 5 µm. (C) Flow cytometric analysis of TCR recycling in control and IFT20KD Jurkat cells, the latter either as such or transiently transfected with a construct encoding Rab8-CA with or without GFP-tagged IFT20. The data, which for each time point refer to duplicate samples from three independent experiments, are presented as the percentage of the internalized receptors that had recycled to the cell surface (mean±s.d.). A representative immunoblot showing endogenous and recombinant Rab8 as well as IFT20 expression is included. *P<0.05; **P<0.01; ***P<0.001.

Based on their colocalization on $Rab11^+$ endosomes, the potential participation of Rab8 in the TCR recycling pathway controlled by IFT20 was addressed by transiently transfecting constitutively active Rab8 in IFT20-knockdown (KD) cells. As shown in Fig. 2A,B, CA-Rab8 did not rescue the TCR recycling defect in IFT20KD cells, indicating that IFT20 is required for Rab8 to promote this process. To formally prove this contention, TCR recycling was analyzed in IFT20KD cells transiently co-transfected with CA-Rab8 and an expression construct encoding IFT20. The high levels of IFT20 mRNA transcribed under the control of the potent CMV enhancer restored IFT20 expression in IFT20KD cells despite the presence of the specific small interfering RNAs (siRNAs) (Fig. 2C). Under these conditions, the TCR recycling defect was rescued in the presence of CA-Rab8 (Fig. 2C), confirming that IFT20 and Rab8 participate in the same pathway. Accordingly, the TCR recycling defect in IFT20KD cells was not exacerbated by DN-Rab8 (Fig. 2A,B). Interestingly, IFT20 overexpression resulted in a statistically significant increase in TCR recycling which was inhibited by DN-Rab8 (data not shown), further supporting the notion that IFT20 and Rab8 act in concert in the regulation of TCR traffic.

Journal of Cell Science (2015) 128, 2541-2552 doi:10.1242/jcs.171652

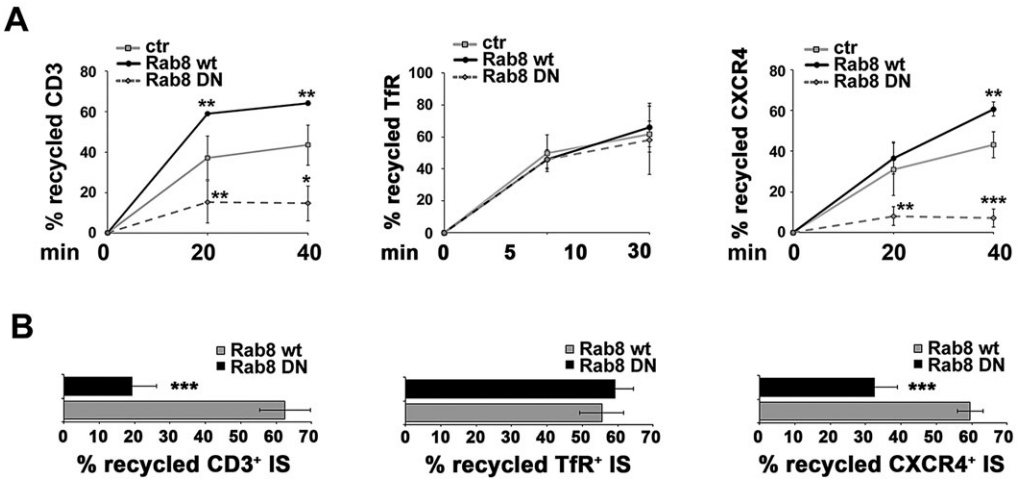

Fig. 3. Rab8 is required for polarized recycling of TCR and CXCR4, but not of TfR, in primary T-cells. (A) Flow cytometric analysis of TCR (left), TfR (middle) and CXCR4 (right) recycling in primary T-cells, transiently transfected with either empty vector (ctr), or wild-type Rab8 (wt) or dominant-negative Rab8 (DN), both tagged with Myc and FLAG. A construct encoding GFP under the control of a constitutive promoter was included in each transfection as control. Analyses were carried out at 24 h post-transfection, gating on GFP^+ live cells. The data, which for each time point refer to triplicate samples from three independent experiments, are presented as the percentage of internalized receptors that have recycled to the cell surface (mean±s.d.). (B) Immunofluorescence analysis under non-permeabilizing conditions of recycled TCR (left), TfR (middle) and CXCR4 (right) in conjugates of primary T-cells, transiently transfected with either empty vector (ctr), or wild-type Rab8 (wt) or dominant negative Rab8 (DN), and SEB-pulsed Raji cells. The data are presented as the percentage of conjugates harboring recycled TCR, TfR or CXCR4 at the immune synapse (mean±s.d.). At least 20 cells were analyzed in each experiment ($n \geq 3$). *P<0.05; **P<0.01; ***P<0.001.

Rab8 regulates both IFT20-dependent and IFT20-independent pathways of receptor recycling

We have recently reported that, in addition to regulating TCR recycling, IFT20 is required for recycling of the TfR, but not of CXCR4 (Finetti et al., 2014), both of which exploit the recycling pathway regulated by Rab11 (Kumar et al., 2011; Maxfield and McGraw, 2004). To further assess the inter-relationship of IFT20 and Rab8 in receptor recycling, the effect of the Rab8 mutants on TfR and CXCR4 recycling was assessed by flow cytometry. Surprisingly, expression of DN-Rab8 did not affect TfR recycling, notwithstanding the fact that, similar to the TCR, this receptor is regulated by IFT20 (Fig 3A; Fig. 4A). By contrast, DN-Rab8 inhibited CXCR4 recycling (Fig. 3A; Fig. 4B), implicating Rab8 in an IFT20-independent recycling pathway for this receptor. Consistent with these findings, recycling of CXCR4, but not of the TfR, was enhanced when cells were transfected with CA-Rab8 (Fig. 3A; Fig. 4A,B). In agreement with the flow cytometric analysis, expression of DN-Rab8 resulted in an accumulation of $CXCR4^+$ endosomes, whereas fewer endosomes were observed in the presence of CA-Rab8 (Fig. 4D). No effect was observed on the intracellular accumulation of TfR^+ endosomes (Fig. 4C).

Similar to control Jurkat cells, neither Rab8 mutant had any impact on the TfR recycling defect observed in IFT20KD cells (Fig. 4A,C). Moreover DN- and CA-Rab8 affected CXCR4 recycling in control and IFT20KD cells to the same extent (Fig. 4B,D). Collectively these results provide evidence that Rab8 participates in both IFT20-dependent and IFT20-independent recycling pathways in T-cells.

Rab8 acts in concert with IFT20 to control polarized TCR recycling to the immune synapse

The association of IFT20 with Rab8 and their interplay in TCR recycling suggests that Rab8 participates in the IFT20-dependent pathway that controls polarized TCR recycling to the immune synapse. To address this issue the localization of Rab8 was first investigated in antigen-specific conjugates of Jurkat cells, with Staphylococcal enterotoxin E (SEE)-loaded Raji cells used as APCs. As expected, the centrosome translocated towards the APC. Under these conditions, Rab8 polarized to the immune synapse together with the centrosome as well as with IFT20 (Fig. 5A).

To understand whether Rab8 is implicated in polarized TCR recycling to the immune synapse, we tracked the fate of internalized TCRs in antigen-specific conjugates of Jurkat T-cells transiently transfected with either empty vector or the construct encoding DN-Rab8. TCR internalization was induced by incubating the cells with anti-CD3 mAb. Cells were then mixed with SEE-loaded APCs, and conjugates were fixed and stained with fluorochrome-labeled secondary antibodies without prior permeabilization. Under these conditions, only the receptors that had recycled to the plasma membrane could be visualized. Confocal imaging of control conjugates showed that the internalized TCRs were concentrated at the immune synapse in control cells, as expected from their polarized recycling. By contrast, a diffuse and weak TCR staining was observed in cells expressing DN-Rab8 (Fig. 5B). Similar results were obtained on primary peripheral blood T-cells (Fig. 3B). Consistent with the defect in polarized TCR recycling, phosphotyrosine signaling at the immune synapse, as well as ERK1/2 phosphorylation induced by SEE-loaded APCs, were impaired in Jurkat cells expressing DN-Rab8 (Fig. 6A,B). Moreover, expression of DN-Rab8 in primary T-cells resulted in a defective response to SEB-loaded APC, as assessed by expression of the activation marker CD69 and production of the cytokine IL-2 (Fig. 6C,D).

Rab8 regulates the IFT20-independent pathway of polarized CXCR4 recycling, but not the IFT20-dependent pathway of polarized TfR recycling

The TfR has been shown to undergo polarized recycling to the immune synapse (Batista et al., 2004), which has been proposed to contribute to immune synapse formation and stability by concentrating the associated CD3ζ (also known as CD247) to this location (Salmeron et al., 1995). Moreover, we have recently shown that polarized recycling is responsible, at least in part, for CXCR4 clustering at the immune synapse (Finetti et al., 2014). The fate of

Journal of Cell Science (2015) 128, 2541-2552 doi:10.1242/jcs.171652

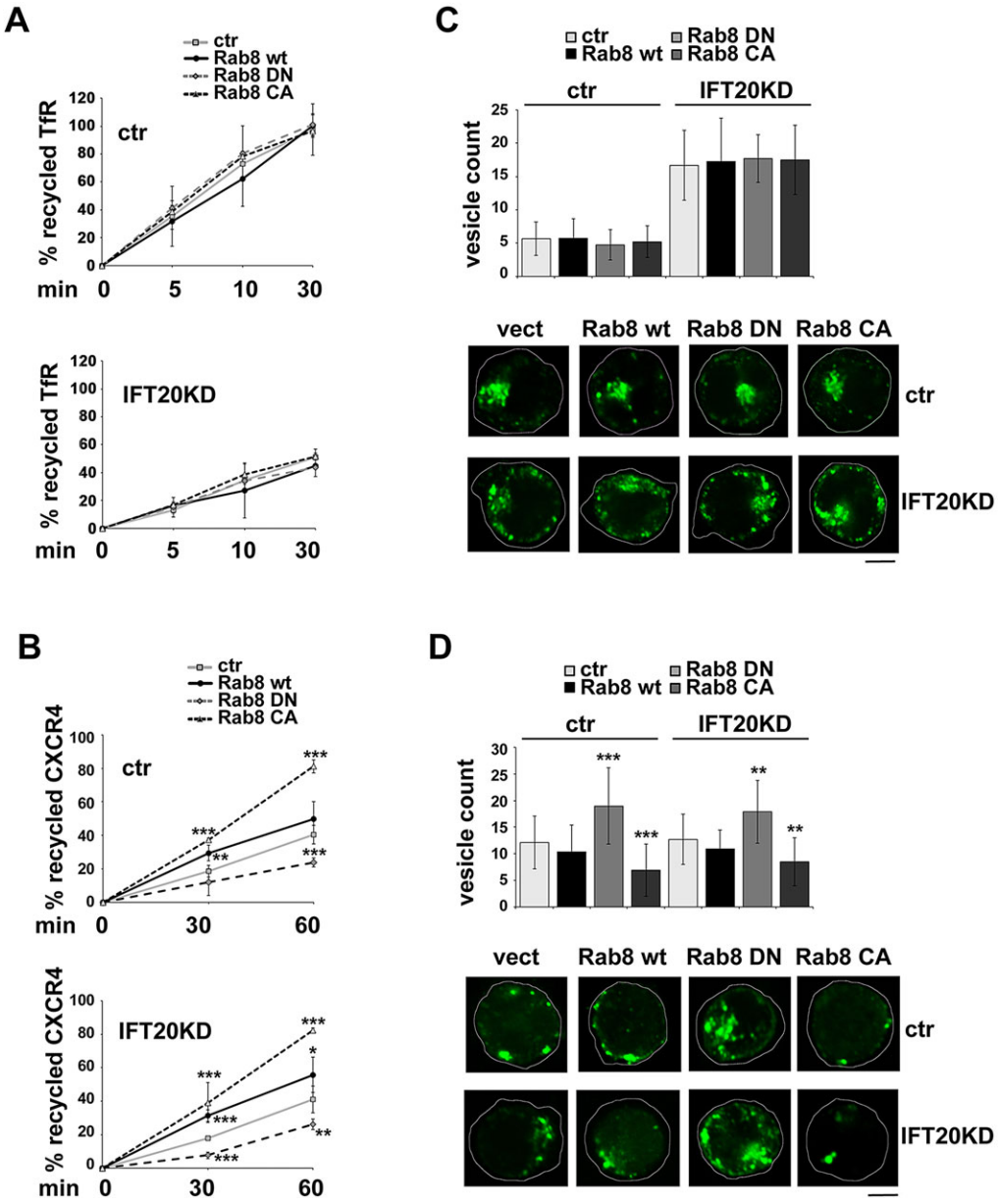

Fig. 4. Rab8 is implicated in IFT20-dependent and -independent pathways of receptor recycling in T-cells. (A,B) Flow cytometric analysis of TfR (A) or CXCR4 (B) recycling in control and IFT20KD Jurkat cells, transiently transfected with either empty vector (ctr), or wild-type Rab8 (wt), dominant-negative Rab8 (DN) or constitutively active Rab8 (CA). A construct encoding GFP under the control of a constitutive promoter was included in each transfection as control. Analyses were carried out at 24 h post-transfection, gating on GFP^+ live cells. The data, which for each time point refer to triplicate samples from three independent experiments, are presented as the percentage of internalized receptors that have recycled to the cell surface (mean±s.d.). (C,D) Counts of vesicles containing internalized TfR (C) or CXCR4 (D) in control and IFT20KD Jurkat cells transiently transfected with wild-type Rab8 or the respective mutants. At least 60 cells were analyzed for each marker ($n \geq 3$). The data are presented as number of labeled vesicles in individual medial confocal sections (mean±s.d.). Representative images are shown. Scale bars: 5 µm. *P<0.05; **P<0.01; ***P<0.001.

internalized TfR and CXCR4 in cells expressing DN-Rab8 was determined by immunofluorescence in conjugates of Jurkat cells with SEE-loaded APC under non-permeabilizing conditions. Consistent with the proposed role for Rab8 in CXCR4 but not TfR recycling, recycling of CXCR4 to the immune synapse was impaired in the presence of DN-Rab8, which, by contrast, did not affect polarized TfR recycling (Fig. 5B). Hence, Rab8 and IFT20 participate individually or in combination in the pathways that control recycling of specific receptors to the T-cell immune synapse.

Rab8 regulates the final steps of TCR recycling to the immune synapse

We have previously shown that TCR^+ endosomes fail to polarize to the immune synapse in the absence of IFT20 (Finetti et al., 2009). Given that the centrosome translocates normally towards the T-cell–APC contact under these conditions (Finetti et al., 2009), this suggests that IFT20 is involved at an early step in the TCR recycling pathway, which we have identified as the sorting or trafficking from early endosomes (Finetti et al., 2014). To map Rab8 in the IFT20-dependent pathway that controls polarized TCR recycling we tracked internalized TCR–CD3 complexes undergoing recycling in antigen-specific conjugates of Jurkat cells transiently transfected with the DN-Rab8 mutant under permeabilizing conditions. Remarkably, imaging of the T-cell–APC conjugates showed that, notwithstanding the defect in TCR recycling to the immune synapse in cells expressing DN-Rab8, the endosomes containing internalized TCRs polarized normally to the immune synapse (Fig. 7A), which does not occur with IFT20KD cells, where polarization failed to occur (Finetti et al., 2009). Hence, when the activity of Rab8 is inhibited, recycling endosomes containing internalized TCRs are still able to polarize close to the T-cell–APC interface but fail to deliver the receptor cargo to the immune synapse, implying that Rab8 is involved in the last steps of TCR recycling to the immune synapse membrane. In support of a function for Rab8 downstream of the polarization to the centrosome of endosomes containing internalized receptors, such as CXCR4, that depend on Rab8 for recycling (Fig. 4B,C), similar results were

Journal of Cell Science (2015) 128, 2541-2552 doi:10.1242/jcs.171652

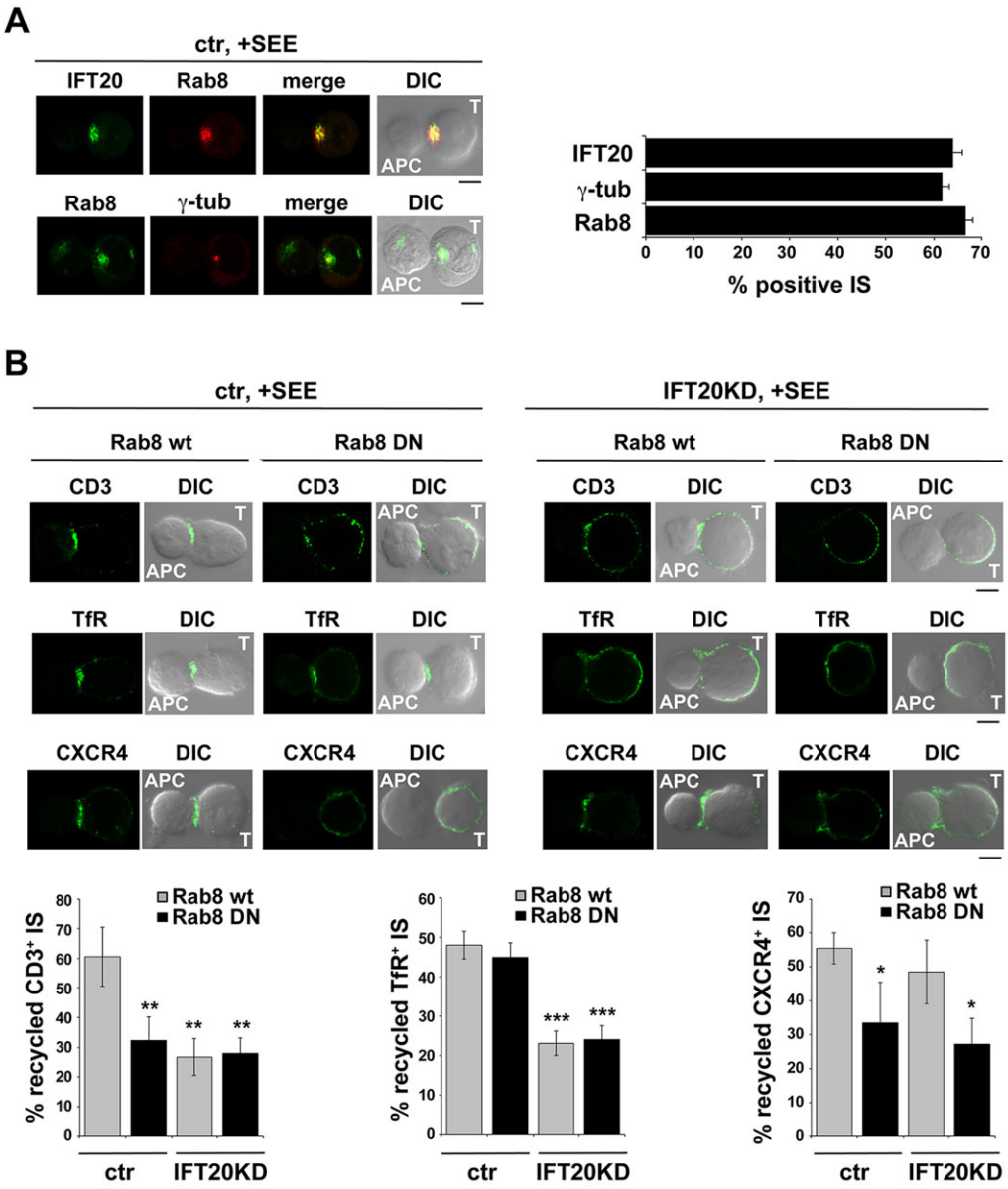

Fig. 5. Rab8 controls IFT20-dependent TCR recycling and IFT20-independent CXCR4 recycling to the immune synapse. (A) Immunofluorescence analysis of Rab8, IFT20 and γ-tubulin in conjugates of Jurkat cells (labeled T), transiently transfected with either empty vector (ctr), or wild-type Rab8 (wt) or dominant-negative Rab8 (DN), and SEE-pulsed Raji cells (labeled APC). The histogram shows the percentage of conjugates harboring Rab8, IFT20 or γ-tubulin at the immune synapse (mean±s.d.). At least 200 cells were analyzed for each marker. Representative images (medial optical sections) are shown. (B) Immunofluorescence analysis under non-permeabilizing conditions of recycled TCR (top), TfR (middle) and CXCR4 (bottom) in conjugates of control or IFT20KD Jurkat cells, transiently transfected with either wild-type Rab8 (wt) or dominant negative Rab8 (DN), and SEE-pulsed Raji cells. The data are presented as the percentage of conjugates harboring recycled TCR, TfR or CXCR4 at the immune synapse (mean±s.d.). At least 50 cells were analyzed in each experiment ($n \geq 3$). *$P<0.05$; ***$P<0.001$; **$P<0.01$. Representative images are shown. Scale bars: 5 µm.

obtained not only for TfR, which is Rab8-independent (Fig. 4A,C), but also for CXCR4 (Fig. 7A).

Rab8 is required for recruitment of the v-SNARE VAMP-3 to the immune synapse

The final steps of delivery of receptor cargo from recycling endosomes to the plasma membrane are dependent on the recruitment of a specific v-SNARE that promotes membrane fusion following its interaction with a cognate target (t)-SNARE at the plasma membrane. During immune synapse formation, both the t-SNAREs syntaxin 4 and SNAP-23 and the v-SNAREs VAMP-3 and VAMP-7 are mobilized to the immune synapse (Das et al., 2004; Larghi et al., 2013). Of these, VAMP-3 has been demonstrated to colocalize with TCR–CD3 complexes undergoing polarized recycling and to be required for their accumulation at the immune synapse (Das et al., 2004).

We addressed the role of Rab8 in VAMP-3 recruitment in Jurkat cells transiently co-transfected with a construct encoding GFP-tagged VAMP-3 and a construct encoding either wild-type or DN-Rab8. Cells were used to form antigen-specific conjugates and analyzed by confocal microscopy. VAMP-3 was found to cluster to the immune synapse in control antigen-specific conjugates, as expected (Fig. 7B). The immune synapse localization of VAMP-3 was impaired in antigen-specific conjugates of T-cells expressing DN-Rab8 (Fig. 7B). However, under these conditions the t-SNARE syntaxin 4 clustered normally at the immune synapse (Fig. 7C). Hence, Rab8 is required for VAMP-3 polarization to the immune synapse, suggesting a role for Rab8 in VAMP-3 recruitment. This possibility was addressed in co-immunoprecipitation assays. As shown in Fig. 7D, Rab8 co-precipitated with VAMP-3, indicating that these proteins are able to interact.

VAMP-3 is required for ciliogenesis and ciliary targeting of the protein Smo

The regulation of polarized TCR recycling to the immune synapse by Rab8, which together with the IFT system is essential for ciliogenesis, highlights the similarities between these structures. We asked whether VAMP-3, which our data identify as a Rab8 effector in T-cells, might be implicated in ciliary assembly, using NIH-3T3 as a ciliated cell model. VAMP-3 was found to localize to a vesicular compartment at

Journal of Cell Science (2015) 128, 2541-2552 doi:10.1242/jcs.171652

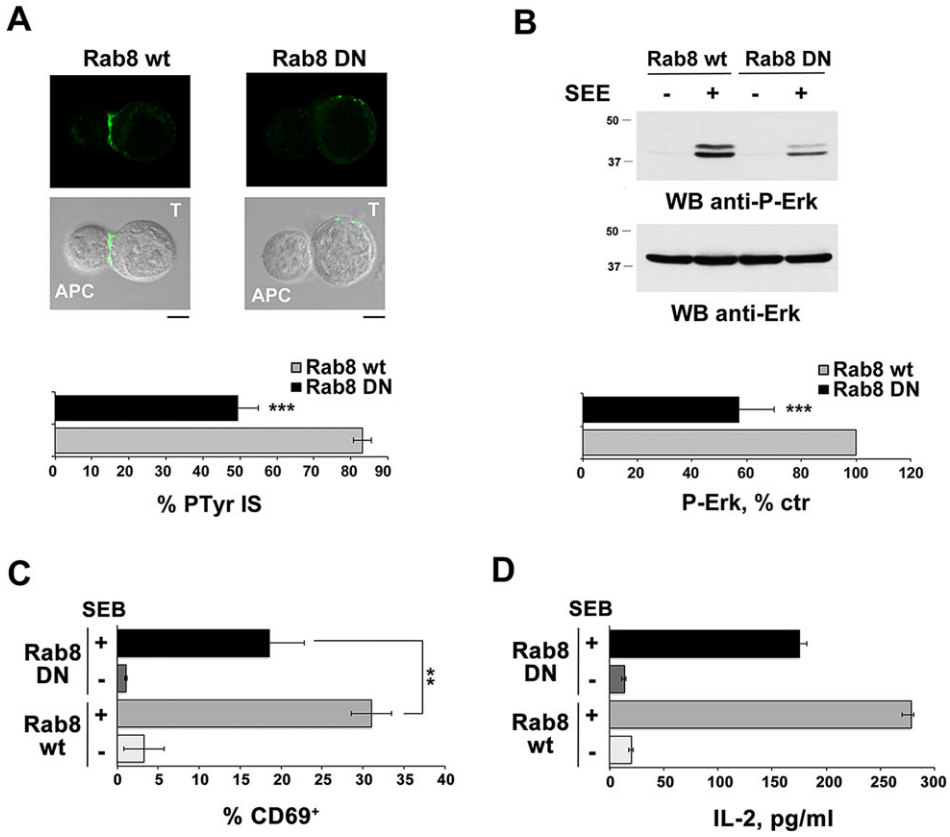

Fig. 6. Rab8 is required for T-cell activation. (A) Immunofluorescence analysis of tyrosine phosphoproteins (PTyr) in conjugates of Jurkat cells (labeled T), transiently transfected with either wild-type Rab8 (wt) or dominant negative Rab8 (DN), and SEE-pulsed Raji cells (labeled APC). Quantification (%, mean±s.d., $n \geq 3$) of conjugates with PTyr staining at the immune synapse are shown below the representative images. At least 300 cells were analyzed for each marker. Scale bars: 5 µm. ***$P<0.001$. (B) Immunoblot analysis of ERK1/2 phosphorylation in lysates from Jurkat cells transiently transfected with either wild-type Rab8 (wt) or dominant negative Rab8 (DN), and incubated with SEE-pulsed Raji cells. The migration of molecular mass markers is indicated. The histogram shows the quantification of the phosphorylated ERK1/2 signal, normalized to ERK2 (mean±s.d., $n=3$; the phosphorylated ERK1/2 level in activated wt Rab8-expressing cells taken as 100%). (C) Flow cytometric analysis of surface CD69 in primary T-cells transiently transfected with either wild-type Rab8 (wt) or dominant-negative Rab8 (DN), and incubated for 16 h with SEB-loaded Raji B cells. Cells were co-stained for CD19 (expressed only by Raji cells) and the analysis was carried out gating on CD19-negative cells. The data are expressed as the percentage of $CD69^+$ T-cells (mean±s.d.). The analysis was carried out in triplicate on three donors. (D) ELISA quantification of IL-2 in culture supernatants of primary T-cells transiently transfected with either wild-type Rab8 (wt) or dominant negative Rab8 (DN), and incubated for 30 h with SEB-loaded Raji B cells The data are presented as pg/ml (mean±s.d.). The analysis was carried out in triplicate on three donors. *$P<0.05$; **$P<0.01$; ***$P<0.001$.

the base of the primary cilium, as assessed in cells transiently transfected with the construct encoding GPF-tagged VAMP-3 and stained for Rab8, which is known to concentrate in the cilium (Fig. 8A).

VAMP-3 depletion by RNA interference resulted in a significant reduction in ciliary length (Fig. 8B), indicating that VAMP-3 participates in the pathway that controls this process. Moreover the localization of the receptor protein Smo, which localizes to the ciliary membrane in response to hedgehog signaling (Wong and Reiter, 2008) was found to be compromised in VAMP-3-depleted NIH-3T3 cells, as assessed in cells transiently transfected with a construct encoding GFP-tagged Smo (Fig. 8C), which is constitutively localized to the cilium when overexpressed (Wu et al., 2012). Co-immunoprecipitation assays showed that, similar to in T-cells, Rab8 interacted with VAMP-3 (Fig. 8D), suggesting that this v-SNARE is involved in the ciliary targeting of endosomes carrying Smo cargo. Hence, VAMP-3 is a Rab8 effector that regulates receptor traffic not only to the immune synapse, but also to the primary cilium.

DISCUSSION

The data presented in this paper, which complement the recent identification of Rab8 in TCR^+ endosomes (Soares et al., 2013), provide the first evidence of a role for Rab8 as a central regulator of TCR recycling in T-cells, which contributes, as such, to immune synapse assembly and T-cell activation. Rab8 has been previously implicated in receptor recycling during polarized cell morphogenesis (Peranen, 2011). A functional link between Rab8 and the recycling compartment in protein transport to the ciliary membrane has moreover been established with the finding that Rabin8 interacts with GTP-bound Rab11 and is carried to pericentrosomal Rab8 at the base of the cilium by $Rab11^+$ vesicles (Westlake et al., 2011). Our results, which demonstrate that Rab8 is a new component of the TCR trafficking pathway regulated by the IFT system in T-cells, provide evidence that Rab8 is implicated in endosome recycling not only in polarized but also in the non-polarized quiescent T-cells, and moreover underscore its link with the machinery that controls ciliogenesis in a cell type lacking a primary cilium.

The results obtained on control and IFT20KD cells transiently transfected with the Rab8 mutants indicate that Rab8 and IFT20 act in concert in regulating TCR recycling, and suggest that IFT20 is involved at an early step and Rab8 at a later step in the pathway. This notion is supported by the fact that, whereas polarized recycling of the TCR is similarly impaired when the function of either IFT20 or Rab8 is disrupted, the endosomes carrying internalized TCRs fail to

Journal of Cell Science (2015) 128, 2541-2552 doi:10.1242/jcs.171652

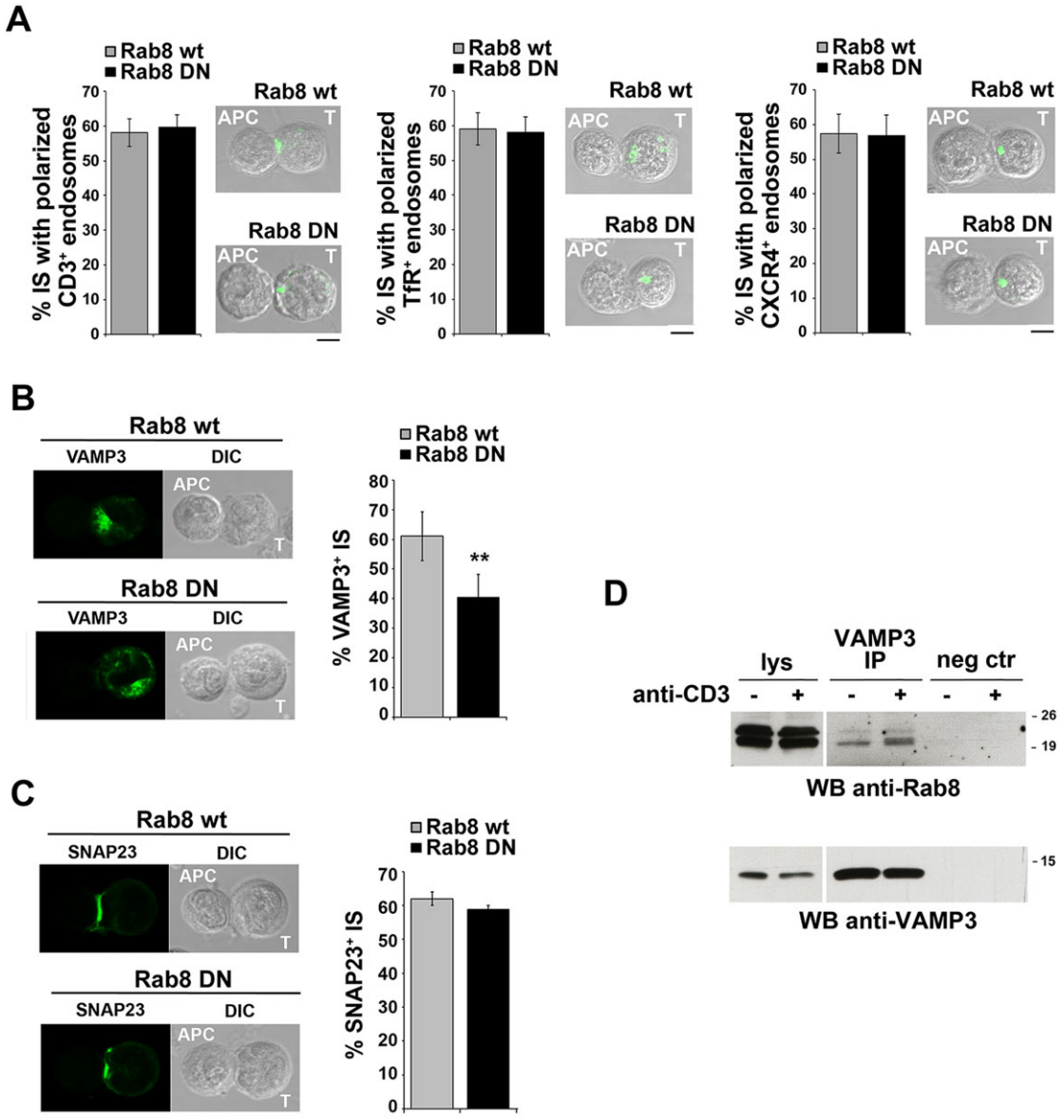

Fig. 7. Rab8 is required for VAMP-3 recruitment to the immune synapse. (A) Immunofluorescence analysis of recycling TCR, TfR and CXCR4 in permeabilized conjugates of Jurkat cells (labeled T), transiently transfected with either wild-type Rab8 (wt) or dominant-negative Rab8 (DN), and SEE-pulsed Raji cells (labeled APC). The histograms show the percentage of conjugates with endosomes containing internalized TCR, TfR or CXCR4 fully polarized at the immune synapse. At least 200 cells were analyzed for each sample (n=3). Representative images are shown. (B,C) Immunofluorescence analysis of GFP-tagged VAMP-3 (B) or SNAP-23 (C) in conjugates of Jurkat cells, transiently transfected with either wild-type Rab8 (wt) or dominant-negative Rab8 (DN), and SEE-pulsed Raji cells. The histograms show the percentage of conjugates with VAMP-3 (B) or SNAP-23 (C) polarization at the immune synapse. At least 300 cells were analyzed for each sample (n=3). Representative images are shown. (D) Immunoblot analysis of VAMP-3-specific immunoprecipitates (IP) from lysates of Jurkat cells, transiently transfected with wild-type Rab8 (wt) or dominant-negative Rab8 (DN), either unstimulated or activated for 10 min by TCR cross-linking. Preclearing controls are included in each blot (neg ctr). Total cell lysates were included in each gel to identify the migration of the proteins tested. The immunoblot shown is representative of three independent experiments. A shorter exposure of the total lysates is shown. The migration of molecular mass markers is indicated.

polarize in cells lacking IFT20 (Finetti et al., 2014), yet they polarize normally in cells expressing DN-Rab8 where only the final step of delivery to the immune synapse membrane is compromised. We have shown that IFT20 interacts with Rab5 and is required for TCR trafficking from early endosomes (Finetti et al., 2014). The implication of IFT20 at an early step in TCR recycling is likely to account for the observation that the TCR recycling defect in IFT20KD cells cannot be rescued by expression of CA-Rab8. Based on the colocalization of IFT20 with both Rab8 and Rab11, it could be hypothesized that, after tagging the receptors to be recycled during their transit through the early endosomes and allowing their transit to Rab11$^+$ endosomes, IFT20 could functionally interact with Rab8, thereby also participating in the final step of delivery of the TCR cargo to the plasma membrane. A dual role at different steps of endosome recycling has been recently documented for Rab11, which has been shown to regulate not only receptor trafficking to the perinuclear recycling compartment (Stenmark, 2009) but also vesicle exocytosis at the plasma membrane in concert with the exocyst (Takahashi et al., 2012; Zhang et al., 2004).

Our results provide evidence that Rab8 also participates in the pathway that controls CXCR4 recycling, but that this does not apply to the TfR, despite the fact that both receptors associate with Rab11$^+$

Journal of Cell Science (2015) 128, 2541-2552 doi:10.1242/jcs.171652

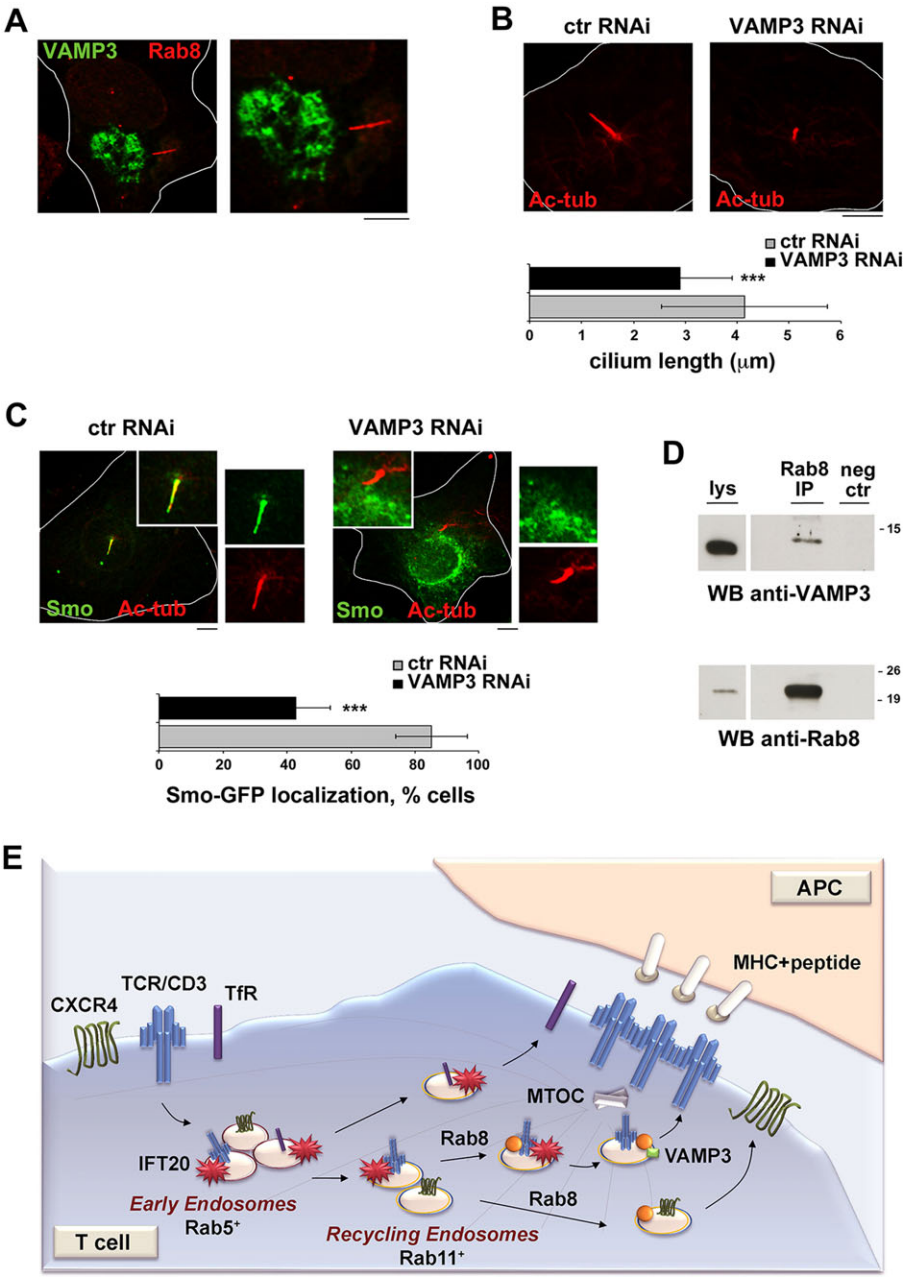

Fig. 8. VAMP-3 is required for ciliary growth and ciliary targeting of Smo in ciliated cells. (A) Immunofluorescence analysis of VAMP-3 (green) and Rab8 (red) localization in NIH3T3 cells transiently transfected with a construct encoding GFP-tagged VAMP-3. The relevant compartment in the image is shown at a higher magnification (1.75×) on the right. Scale bar: 5 μm. (B) Quantification of ciliary length (μm) in NIH-3T3 cells transiently transfected with VAMP-3-specific siRNAs (VAMP3 RNAi giving ~50% VAMP-3KD) or non-relevant control siRNAs (ctr RNAi) and stained for acetylated tubulin. At least 200 cilia were analyzed for each transfectant (n=3). Scale bar: 5 μm. (C) Immunofluorescence analysis of Smo (green) localization in NIH-3T3 cells, transiently co-transfected with GFP-tagged Smo and either VAMP-3-specific siRNAs or non-relevant control siRNAs. The relevant section of the image is shown at a higher magnification. The histogram shows the quantification (%, mean±s.d.) of cells with ciliary localization of Smo-GFP (≥20 cells per sample, n=3). ***P<0.001. Scale bar: 5 μm. (D) Immunoblot analysis of Rab8-specific immunoprecipitates from lysates of NIH-3T3 cells. A preclearing control was included in each blot (neg ctr). A total cell lysate was included in each gel to identify the migration of the proteins tested. The immunoblot shown is representative of three independent experiments. A shorter exposure of the total lysate is shown. The migration of molecular mass markers is indicated. (E) Scheme summarizing the Rab8-dependent and -independent pathways that regulate receptor traffic to the immune synapse.

endosomes (Kumar et al., 2011; Maxfield and McGraw, 2004). This suggests that Rab8 might have a more restricted function in controlling receptor recycling compared to the general regulators Rab11 and Rab4. It should be, however, underlined that the TfR recycles both through the slow route regulated by Rab11 and the fast route regulated by Rab4 (Maxfield and McGraw, 2004). Hence, it could be hypothesized that the Rab4-dependent pathway might bypass a potential block in the Rab11-dependent pathway imposed by DN-Rab8, resulting in a lack of effect for this mutant on TfR recycling. In support of this notion, expression of DN-Rab8 was found to result in the failure of the TfR to accumulate in the pericentriolar region and in cell surface protrusions at the leading edge during HT1080 fibrosarcoma cell morphogenesis, but did not affect transferrin recycling (Hattula et al., 2006). Of note, we have shown that TfR, but not CXCR4 recycling, is also dependent on IFT20 and other components of the IFT system (Finetti et al., 2014). Taken together with the involvement of both Rab8 and IFT20 in TCR recycling, these data highlight the existence of distinct pathways of receptor recycling defined by the alternative combinatorial usage of various components of the recycling machinery, depending on the identity of the recycling receptor. Interestingly, we found that, unlike in T-cells, IFT20 is not required for TfR recycling in B-cells (L.P. and C.T.B., unpublished results), suggesting the existence of multiple cell-type-specific recycling pathways for this receptor.

The identity of the SNAREs implicated in trafficking to the immune synapse has only recently started to be investigated. Polarized TCR recycling has been demonstrated to depend on a tetanus-toxin-sensitive v-SNARE, which, based on its colocalization with the TCR, has been proposed to be VAMP-3 (Das et al., 2004). Moreover a colocalization of CD3ζ with Rab8 and Ti-VAMP (also known as VAMP7) has been recently described (Soares et al., 2013), suggesting that Rab8 might interact with the v-SNAREs to regulate TCR traffic. Here, we demonstrate that this link indeed exists by

Journal of Cell Science (2015) 128, 2541-2552 doi:10.1242/jcs.171652

showing that VAMP-3 fails to be recruited to the immune synapse when the function of Rab8 is compromised. This immune-synapse-proximal role of Rab8 is consistent with the failure of recycling TCRs to be delivered to the plasma membrane after their mobilization to the centrosome.

Interestingly, the reduction in ciliary length observed in NIH-3T3 cells depleted of VAMP-3 reveals a role for this v-SNARE in the trafficking events that regulate the growth of this organelle. The notion of the primary cilium as a specialized form of polarized membrane transport has been suggested based on bioinformatic analyses that have highlighted structural similarities between the components of the IFT system and membrane coatamers (Jekely and Arendt, 2006). The discovery of the BBSome, which cooperates with the IFT system in ciliogenesis by promoting the Rab8-dependent protein traffic to the ciliary membrane (Nachury et al., 2010), has provided experimental support to this contention and paved the way to the dissection of a trafficking pathway that involves the participation of recycling endosomes (Westlake et al., 2011). One of the open questions is whether the ciliary membrane proteins are recruited to the cilium by lateral mobility, assisted by the IFT system and/or the BBSome to cross the physical barrier of the transition zone at the base of the cilium, or whether they are alternatively directly transported as endosomal cargos to this location. The latter scenario is strongly supported by the finding that both the t-SNAREs syntaxin-3 and SNAP-25, and the v-SNARE VAMP-7 are required for efficient ciliogenesis (Mazelova et al., 2009; Szalinski et al., 2014). Our results identify VAMP-3 as a new player in the pathway that regulates this process. Of note, VAMP-3 also regulates Smo trafficking to the cilium. Vesicular trafficking is centrally implicated in the dynamic ciliary localization of this receptor, on which Hedgehog signaling crucially depends, as underscored by the variety of Rab and Arl GTPases that are required for the ciliary targeting of Smo, including Rab8, Rab23 and Arl6 (Boehlke et al., 2010; Zhang et al., 2011). VAMP-3 is the first SNARE to be identified in this pathway. Although its interaction with Rab8 suggests that VAMP-3 acts as an effector of Rab8, likely promoting the delivery of endosome-associated Smo to the base of the cilium, their distinct subcellular localizations, at the base and inside the cilium, respectively, indicate that the proteins dissociate once they have reached this location.

In conclusion, our results identify Rab8 downstream of IFT20 in the pathway that regulates TCR recycling, where its function is to recruit VAMP-3 to promote the fusion with the immune synapse membrane of endosomes carrying TCR cargo that have polarized towards the APC (Fig. 8E). Taken together with findings showing that IFT20 and other IFT proteins are involved in TCR trafficking and immune synapse assembly (Finetti et al., 2009, 2014), as well as the function of VAMP-3 as a Rab8 effector in the control of Smo trafficking to the primary cilium, these results further highlight the remarkable conservation in the pathways that orchestrate immune synapse formation and ciliogenesis.

MATERIALS AND METHODS

Cells, plasmids, transfections, antibodies and reagents

Cells included Jurkat T-cells, Raji B cells and NIH3T3 murine fibroblasts, as well as normal T-cells purified from peripheral blood from healthy donors (informed consent was obtained according to the Declaration of Helsinki) by Ficoll gradient centrifugation. The latter were expanded by stimulation with Staphylococcal enterotoxin B (SEB) for 7–10 days in order to increase the number of antigen-specific T-cells. Stable control and IFT20KD Jurkat lines were as previously described (Finetti et al., 2009). Human wild-type, T22N (DN) and Q77L (CA) Rab8 in p3XFLAG-myc-CMV-26 (Sigma-Aldrich) (Follit et al., 2010), pCMV-EGFP-C3-Rab11 (kindly provided by M. Zerial, Max Planck Institute of Molecular Cell Biology and Genetics, Germany), pCMV-EGFP-C3-VAMP3, pCMV-EGFP-C3-SNAP23 (kindly provided by A. Alcover, Lymphocyte Cell Biology Unit, Institut Pasteur, France, and C. Hivroz, Pavillon Pasteur, Institut Curie, France), pmaxGFP, pJAF2.13 (IFT20GFP) (Follit et al., 2006) and pEGFP-mouse Smoothened (pEGFP-mSmo) (Addgene plasmid #25395) or short hairpin RNA (shRNA) constructs for human or mouse VAMP-3 (OriGene Technologies, Inc) were used. Jurkat cells were transfected by electroporation. Normal T-cells were transiently transfected by nucleofection using the Amaxa nucleofector device (Amaxa Biosystems) and the conditions for T-cell transfection recommended by the manufacturer. Transient transfections of NIH-3T3 cells were performed using Turbofectamine (ThermoScientific). Cells were analyzed 24 h post-transfection, with the exception of VAMP-3KD NIH-3T3 cells, where assays were carried out after 72 h.

Polyclonal anti-IFT20 antibodies were as previously described (Pazour et al., 2002). IgG from OKT3 (anti-CD3ε) hybridoma supernatants was purified using Mabtrap (Amersham Biosciences, Inc) and titrated by flow cytometry. Anti-TfR mAb (hybridoma OKT9) was generously provided by A. Alcover, anti-CXCR4 antibodies by J. Hoxie (Department of Medicine, University of Pennsylvania School of Medicine, PA), Leukosite and the MRC AIDS Reagent Project. Anti-phosphotyrosine antibodies were purchased from Upstate Biotechnology (Temecula, CA); anti-GFP mAb and anti-GFP polyclonal antibodies (pAb) were from Invitrogen (Milan, Italy); anti-actin mAb was from Merck Millipore (Billerica, MA); anti-γ tubulin and anti-acetylated tubulin mAb were from Sigma-Aldrich (St Louis, MO); anti-phosphorylated-p44/42 MAPK (ERK1/2), anti-Rab8 and anti-Rab11 pAbs were from Cell Signaling Technology (Beverly, MA); anti-Erk2 pAb and anti-Rab8 mAb were from Santa Cruz Biotechnology (Santa Cruz, CA, USA); anti-VAMP-3 pAb was from Abcam (Cambridge, UK). Unlabeled secondary antibodies were from Cappel (ICN Pharmaceuticals Inc, CA), secondary peroxidase-labeled antibodies from Amersham Biosciences. Alexa-Fluor-488- and -555-labeled secondary Abs were from Molecular Probes (Invitrogen), phycoerythrin-conjugated anti-mouse-Ig was from eBiosciences (San Diego, CA), allophycocyanin-conjugated CD19 was from BD Biosciences and CD69–FITC from BioLegend (San Diego, CA). Staphylococcal enterotoxins E (SEE) and B (SEB) were purchased from Toxin Technology (Sarasota, FL), Cell Tracker Blue was from Molecular Probes (Invitrogen) and poly-L-lysine from Sigma-Aldrich.

Flow cytometry and immunofluorescence analysis of receptor recycling

Receptor recycling was quantified by flow cytometry as previously described (Finetti et al., 2014). Briefly cells were incubated 30 min on ice with saturating concentrations of mAb specific for each receptor, washed with cold PBS and shifted to 37°C for 15 (TfR) or 60 min (TCR, CXCR4). Cells were acid-stripped, washed and incubated at 37°C to allow recycling of receptor–mAb complexes. Receptor–mAb complexes that had recycled to the cell surface were measured by labeling with fluorochrome-labeled secondary Ig. The data are presented as percentage of the internalized receptors that have recycled to the cell surface, calculated as described previously (Finetti et al., 2014). Flow cytometry was carried out using a FACScan flow cytometer (Becton Dickinson, San Jose, CA).

Vesicles containing internalized receptors were analyzed by immunofluorescence as described previously (Finetti et al., 2014). Cells were incubated with saturating concentrations of mAb specific for each receptor at 37°C for 2 h, washed to remove excess mAb, allowed to adhere for 15 min on polylysine-coated wells of diagnostic microscope slides (Erie Scientific Company), fixed in 4% paraformaldehyde for 20 min at room temperature and permeabilized in PBS 0.01% Triton X-100 for 20 min at room temperature. Internalized receptor–mAb complexes were labeled using fluorochrome-labeled secondary Ig and visualized by confocal microscopy. The number of vesicles positive for each receptor was determined in individual medial confocal sections using ImageJ as described previously (Finetti et al., 2014).

Conjugate formation, T-cell activation assays

Conjugates between Jurkat cells and SEE-pulsed Raji B cells, or normal T-cells and SEB-loaded Raji cells, were carried out as previously described

(Finetti et al., 2009). TCR, TfR or CXCR4 recycling at the immune synapse were analyzed as described previously (Finetti et al., 2014). Briefly, cells were incubated with mAb specific for each receptor at 37°C for 2 h, acid-stripped, incubated 15 min at 37°C with SEE (or SEB)-pulsed Raji cells and then plated on polylysine-coated wells. Samples were fixed by immersion in methanol for 10 min at −20°C, or analyzed under non-permeabilizing conditions after fixation in 4% paraformaldehyde.

T-cell activation following incubation of primary T-cells (16 h) with Raji cells in the presence or absence of SAg was quantified by flow cytometric analysis of surface CD69, excluding from the analysis the $CD19^+$ Raji cells. Alternatively, IL-2 was measured in culture supernatants using the Human IL-2 Ready-Set-Go! ELISA kit from eBioscience.

Immunofluorescence microscopy and colocalization analyses

Following fixation, samples were washed 5 min in PBS and incubated with primary antibodies overnight at 4°C or 1 h at room temperature. After washing in PBS, samples were incubated for 1 h at room temperature with Alexa-Fluor-488- and -555-labeled secondary antibodies. Confocal microscopy was carried out on a Zeiss LSM700 using a 63× objective. Images were acquired with pinholes opened to obtain 0.8-µm-thick sections. Detectors were set to detect an optimal signal below the saturation limits. Images were processed with Zen 2009 image software (Carl Zeiss, Jena, Germany).

The colocalization analyses were carried out on Jurkat cells as well as normal T-cells transiently transfected with the GFP-tagged Rab11 or IFT20 constructs. The quantitative colocalization analysis of IFT20 and GFP protein signals in the Jurkat transfectants expressing the different GFP-tagged Rab proteins was performed on median optical sections using the zero-crossing procedure as previously described (Perinetti et al., 2009; Finetti et al., 2009). Scoring of conjugates for polarized receptor recycling to the immune synapse in permeabilized or non-permeabilized cells as well as for VAMP-3 and SNAP-23 clustering at the immune synapse in permeabilized cells was based on the concentration of the respective staining solely at the T-cell–APC contact.

The length of cilia was measured using ImageJ on NIH3T3 cells grown to 70–90% confluency and serum-starved for 72 h, followed by fixation and permeabilization by immersion in methanol for 10 min at −20°C and staining with an anti-acetylated tubulin mAb.

Membrane fractionation on iodixanol gradients

Jurkat cell membranes were fractionated by centrifugation on 10–30% iodixanol gradients as previously described (Finetti et al., 2014). 50×10^6 Jurkat T-cells were homogenized by ten passages through a 26-gauge syringe needle, preceded by Dounce homogenization (10 pestle strokes) in 1 ml homogenization medium (0.25 M sucrose, 1 mM EDTA, 10 mM Tris-HCl pH 7.4) in the presence of protease inhibitors. The homogenate was centrifuged at 3000 ***g*** for 5 min at 4°C to remove nuclei and mitochondria, and the supernatant was centrifuged at 68,000 ***g*** for 1 h at 4°C. The microsomal pellet was resuspended in 1.2 ml homogenization medium, mixed 1:1 with 60% iodixanol (Sigma-Aldrich) in buffer diluent (0.25 M sucrose, 6 mM EDTA, 60 mM Tris-HCl pH 7.4), layered on an iodixanol gradient consisting of 1.3 ml 20% iodixanol and 1.2 ml 10% iodixanol in homogenization medium and centrifuged at 350,000 ***g*** for 3 h at 4°C. Ten fractions were collected from the top of the tube and analyzed by SDS-PAGE (equal volumes of each fraction).

Activations, immunoprecipitations and immunoblotting

Activations were performed by incubating Jurkat cells (5×10^7 cells per sample for immunoprecipitation experiments) with saturating concentrations of anti-CD3 mAb and 50 µg/ml secondary Ig for 10 min at 37°C as described previously (Finetti et al., 2009). Activations of Jurkat cells by SEE-pulsed Raji cells were performed as previously described by incubating Jurkat and Raji cells (3×10^6 cells per sample for immunoblotting experiments on total cell lysates) for 15 min at 37°C. For immunoprecipitation experiments on NIH3T3 cells, 5×10^7 cells per sample were used. Cells were lysed in 0.5% Triton X-100 in 20 mM Tris-HCl pH 8, 150 mM NaCl in the presence of protease inhibitors, and postnuclear supernatants were immunoprecipitated using anti-Rab8 or anti-VAMP-3 polyclonal antibodies and protein-A–Sepharose (Amersham). Immunoblotting was carried out using peroxidase-labeled secondary Ig and a chemiluminescence detection kit (Pierce Rockford, IL). Filters were reprobed with control antibodies after stripping. Blots were scanned using a laser densitometer (Duoscan T2500; Agfa, Milan, Italy) and quantified using ImageJ 1.46r (National Institutes of Health, USA).

Statistical analysis

Mean values, standard deviation values and Student's *t*-test (unpaired) were calculated using the Microsoft Excel application. A $P<0.05$ was considered as statistically significant.

Acknowledgements

The authors wish to thank Peter van der Slujis, Andres Alcover, Marino Zerial, Claire Hivroz and Jean-Marie Carpier for useful discussions and for generously providing key reagents, Joel Rosenbaum and John Telford for advice and Sonia Grassini for technical assistance.

Competing interests

The authors declare no competing or financial interests.

Author contributions

F.F., L.P., D.G., C.C., G.P. and C.T.B. designed the experiments and analyzed the data; F.F., L.P., D.G. and C.C. carried out the experiments; G.J.P. provided key reagents; F.F. and C.T.B. wrote the paper.

Funding

The financial support of Telethon - Italy [grant number GGP1102] is gratefully aknowledged. Deposited in PMC for release after 6 months.

References

Batista, A., Millan, J., Mittelbrunn, M., Sanchez-Madrid, F. and Alonso, M. A. (2004). Recruitment of transferrin receptor to immunological synapse in response to TCR engagement. *J. Immunol.* **172**, 6709-6714.

Boehlke, C., Bashkurov, M., Buescher, A., Krick, T., John, A.-K., Nitschke, R., Walz, G. and Kuehn, E. W. (2010). Differential role of Rab proteins in ciliary trafficking: Rab23 regulates smoothened levels. *J. Cell Sci.* **123**, 1460-1467.

Das, V., Nal, B., Dujeancourt, A., Thoulouze, M.-I., Galli, T., Roux, P., Dautry-Varsat, A. and Alcover, A. (2004). Activation-induced polarized recycling targets T cell antigen receptors to the immunological synapse; involvement of SNARE complexes. *Immunity* **20**, 577-588.

Esseltine, J. L., Ribeiro, F. M. and Ferguson, S. S. G. (2012). Rab8 modulates metabotropic glutamate receptor subtype 1 intracellular trafficking and signaling in a protein kinase C-dependent manner. *J. Neurosci.* **32**, 16933-16942.

Finetti, F., Paccani, S. R., Riparbelli, M. G., Giacomello, E., Perinetti, G., Pazour, G. J., Rosenbaum, J. L. and Baldari, C. T. (2009). Intraflagellar transport is required for polarized recycling of the TCR/CD3 complex to the immune synapse. *Nat. Cell Biol.* **11**, 1332-1339.

Finetti, F., Patrussi, L., Masi, G., Onnis, A., Galgano, D., Lucherini, O. M., Pazour, G. J. and Baldari, C. T. (2014). Specific recycling receptors are targeted to the immune synapse by the intraflagellar transport system. *J. Cell Sci.* **127**, 1924-1937.

Follit, J. A., Tuft, R. A., Fogarty, K. E. and Pazour, G. J. (2006). The intraflagellar transport protein IFT20 is associated with the Golgi complex and is required for cilia assembly. *Mol. Biol. Cell* **17**, 3781-3792.

Follit, J. A., Li, L., Vucica, Y. and Pazour, G. J. (2010). The cytoplasmic tail of fibrocystin contains a ciliary targeting sequence. *J. Cell Biol.* **188**, 21-28.

Fooksman, D. R., Vardhana, S., Vasiliver-Shamis, G., Liese, J., Blair, D. A., Waite, J., Sacristan, C., Victora, G. D., Zanin-Zhorov, A. and Dustin, M. L. (2010). Functional anatomy of T cell activation and synapse formation. *Annu. Rev. Immunol.* **28**, 79-105.

Gerges, N. Z., Backos, D. S. and Esteban, J. A. (2004). Local control of AMPA receptor trafficking at the postsynaptic terminal by a small GTPase of the Rab family. *J. Biol. Chem.* **279**, 43870-43878.

Hattula, K., Furuhjelm, J., Tikkanen, J., Tanhuanpaa, K., Laakkonen, P. and Peranen, J. (2006). Characterization of the Rab8-specific membrane traffic route linked to protrusion formation. *J. Cell Sci.* **119**, 4866-4877.

Iezzi, G., Karjalainen, K. and Lanzavecchia, A. (1998). The duration of antigenic stimulation determines the fate of naive and effector T cells. *Immunity* **8**, 89-95.

Jekely, G. and Arendt, D. (2006). Evolution of intraflagellar transport from coated vesicles and autogenous origin of the eukaryotic cilium. *Bioessays* **28**, 191-198.

Kumar, A., Kremer, K. N., Dominguez, D., Tadi, M. and Hedin, K. E. (2011). Galpha13 and Rho mediate endosomal trafficking of CXCR4 into Rab11+ vesicles upon stromal cell-derived factor-1 stimulation. *J. Immunol.* **186**, 951-958.

Larghi, P., Williamson, D. J., Carpier, J.-M., Dogniaux, S., Chemin, K., Bohineust, A., Danglot, L., Gaus, K., Galli, T. and Hivroz, C. (2013). VAMP7

controls T cell activation by regulating the recruitment and phosphorylation of vesicular Lat at TCR-activation sites. *Nat. Immunol.* **14**, 723-731.

Liew, G. M., Ye, F., Nager, A. R., Murphy, J. P., Lee, J. S., Aguiar, M., Breslow, D. K., Gygi, S. P. and Nachury, M. V. (2014). The intraflagellar transport protein IFT27 promotes BBSome exit from cilia through the GTPase ARL6/BBS3. *Dev. Cell* **31**, 265-278.

Liu, H., Rhodes, M., Wiest, D. L. and Vignali, D. A. A. (2000). On the dynamics of TCR:CD3 complex cell surface expression and downmodulation. *Immunity* **13**, 665-675.

Maxfield, F. R. and McGraw, T. E. (2004). Endocytic recycling. *Nat. Rev. Mol. Cell Biol.* **5**, 121-132.

Mazelova, J., Ransom, N., Astuto-Gribble, L., Wilson, M. C. and Deretic, D. (2009). Syntaxin 3 and SNAP-25 pairing, regulated by omega-3 docosahexaenoic acid, controls the delivery of rhodopsin for the biogenesis of cilia-derived sensory organelles, the rod outer segments. *J. Cell Sci.* **122**, 2003-2013.

Nachury, M. V., Loktev, A. V., Zhang, Q., Westlake, C. J., Peranen, J., Merdes, A., Slusarski, D. C., Scheller, R. H., Bazan, J. F., Sheffield, V. C. et al. (2007). A core complex of BBS proteins cooperates with the GTPase Rab8 to promote ciliary membrane biogenesis. *Cell* **129**, 1201-1213.

Nachury, M. V., Seeley, E. S. and Jin, H. (2010). Trafficking to the ciliary membrane: how to get across the periciliary diffusion barrier? *Annu. Rev. Cell Dev. Biol.* **26**, 59-87.

Patino-Lopez, G., Dong, X., Ben-Aissa, K., Bernot, K. M., Itoh, T., Fukuda, M., Kruhlak, M. J., Samelson, L. E. and Shaw, S. (2008). Rab35 and its GAP EPI64C in T cells regulate receptor recycling and immunological synapse formation. *J. Biol. Chem.* **283**, 18323-18330.

Pazour, G. J. and Bloodgood, R. A. (2008). Targeting proteins to the ciliary membrane. *Curr. Top. Dev. Biol.* **85**, 115-149.

Pazour, G. J., Baker, S. A., Deane, J. A., Cole, D. G., Dickert, B. L., Rosenbaum, J. L., Witman, G. B. and Besharse, J. C. (2002). The intraflagellar transport protein, IFT88, is essential for vertebrate photoreceptor assembly and maintenance. *J. Cell Biol.* **157**, 103-114.

Pedersen, L. B. and Rosenbaum, J. L. (2008). Intraflagellar transport (IFT) role in ciliary assembly, resorption and signalling. *Curr. Top. Dev. Biol.* **85**, 23-61.

Peranen, J. (2011). Rab8 GTPase as a regulator of cell shape. *Cytoskeleton* **68**, 527-539.

Perinetti, G., Müller, T., Spaar, A., Polishchuk, R., Luini, A. and Egner, A. (2009). Correlation of 4Pi and electron microscopy to study transport through single Golgi stacks in living cells with super resolution. *Traffic* **10**, 379-391.

Salmeron, A., Borroto, A., Fresno, M., Crumpton, M. J., Ley, S. C. and Alarcon, B. (1995). Transferrin receptor induces tyrosine phosphorylation in T cells and is physically associated with the TCR zeta-chain. *J. Immunol.* **154**, 1675-1683.

Soares, H., Henriques, R., Sachse, M., Ventimiglia, L., Alonso, M. A., Zimmer, C., Thoulouze, M.-I. and Alcover, A. (2013). Regulated vesicle fusion generates signaling nanoterritories that control T cell activation at the immunological synapse. *J. Exp. Med.* **210**, 2415-2433.

Stenmark, H. (2009). Rab GTPases as coordinators of vesicle traffic. *Nat. Rev. Mol. Cell Biol.* **10**, 513-525.

Szalinski, C. M., Labilloy, A., Bruns, J. R. and Weisz, O. A. (2014). VAMP7 modulates ciliary biogenesis in kidney cells. *PLoS ONE* **9**, e86425.

Takahashi, S., Kubo, K., Waguri, S., Yabashi, A., Shin, H.-W., Katoh, Y. and Nakayama, K. (2012). Rab11 regulates exocytosis of recycling vesicles at the plasma membrane. *J. Cell Sci.* **125**, 4049-4057.

Wei, Q., Zhang, Y., Li, Y., Zhang, Q., Ling, K. and Hu, J. (2012). The BBSome controls IFT assembly and turnaround in cilia. *Nat. Cell Biol.* **14**, 950-957.

Westlake, C. J., Baye, L. M., Nachury, M. V., Wright, K. J., Ervin, K. E., Phu, L., Chalouni, C., Beck, J. S., Kirkpatrick, D. S., Slusarski, D. C. et al. (2011). Primary cilia membrane assembly is initiated by Rab11 and transport protein particle II (TRAPPII) complex-dependent trafficking of Rabin8 to the centrosome. *Proc. Natl. Acad. Sci. USA* **108**, 2759-2764.

Wong, S. Y. and Reiter, J. F. (2008). The primary cilium at the crossroads of mammalian hedgehog signaling. *Curr. Top. Dev. Biol.* **85**, 225-260.

Wu, V. M., Chen, S. C., Arkin, M. R. and Reiter, J. F. (2012). Small molecule inhibitors of Smoothened ciliary localization and ciliogenesis. *Proc. Natl. Acad. Sci. USA* **109**, 13644-13649.

Zhang, X.-M., Ellis, S., Sriratana, A., Mitchell, C. A. and Rowe, T. (2004). Sec15 is an effector for the Rab11 GTPase in mammalian cells. *J. Biol. Chem.* **279**, 43027-43034.

Zhang, Q., Nishimura, D., Seo, S., Vogel, T., Morgan, D. A., Searby, C., Bugge, K., Stone, E. M., Rahmouni, K. and Sheffield, V. C. (2011). Bardet-Biedl syndrome 3 (Bbs3) knockout mouse model reveals common BBS-associated phenotypes and Bbs3 unique phenotypes. *Proc. Natl. Acad. Sci. USA* **108**, 20678-20683.

Journal of Cell Science